Grain size sorting on tidal sandbanks

R. Wemmenhove

Water Engineering and Management, Faculty of Engineering Technology, University of Twente, P.O. Box 217, 7500 AE, Enschede, The Netherlands.
E-mail address: r.wemmenhove@math.rug.nl

Abstract
The spatial segregation of different grain size fractions on tidal sandbanks has not been modelled extensively up to now. The motion of water and sediment around tidal sandbanks is quite complex, the model presented in this article considers a sea bed consisting of two grain size classes that are subject to a tidal flow. The model resolves the hydrodynamics and sediment motion on the fast tidal timescale, allowing for an asymmetrical tidal flow with an M0-, an M2- and an M4-component. Coarse sediment particles are concentrated on the lee side of a migrating sandbank due to the parametrization of the hiding effect.

1. Introduction
The bottom of shallow coastal seas like the North Sea is often covered with regular patterns of bed forms. Tidal sandbanks are the largest of these bed forms, having a wavelength up to 10 kilometers and a height up to tens of meters. They mainly consist of noncohesive sand with a grain diameter of 100 μm to 500 μm. Despite considerable research advances in the last years, the development of tidal sandbanks is still not fully understood. The physical processes concerning the morphodynamics of tidal sandbanks are complex, they are determined by the complex interaction of tidal currents, waves and sediment motion.
In the past years, most process-based research on tidal sandbanks has taken only uniform sediment into account. The process of formation of sandbanks has been studied most thoroughly during the last 20 years. (Huthnance, 1982) showed that sandbanks may arise as instabilities of a flat seabed subject to a tidal flow and bedload transport. His model could predict a preferred wavelength and orientation for tidal sandbanks. His results have been extended by (De Vriend, 1990) and (Hulscher et al., 1993) including suspended load, surface waves and an elliptical tidal forcing. The theories cited here are linear stability analyses and are therefore only valid when sandbanks do not grow too large compared with the water depth.
The effects of nonuniform sediment on tidal sandbanks have not been investigated extensively up to now. Previous model studies on sediment sorting have mainly focused on fluvial conditions. (Ribberink, 1987) analyzed the effect of nonuniform sediment on the development of river dunes, his results have been extended by (Blom, 2003). (Walgreen, 2003) studied the effect of nonuniform sediment on the morphodynamics of shoreface-connected sand ridges and on tidal sand ridges.
In this paper the model approach of (Hulscher et al., 1993) is extended to take effects of nonuniform sediment into account. The impact of nonuniform sediment on the development of sandbanks is part of the research. Furthermore, predicting the spatial segregation of different grain size fractions could clarify morphological developments.
The paper starts with a description of the model structure. After a formulation of the hydrodynamics and sediment motion a framework is built for the morphodynamics of tidal sandbanks. This framework is used to generate model results for symmetrical and asymmetrical tidal conditions.

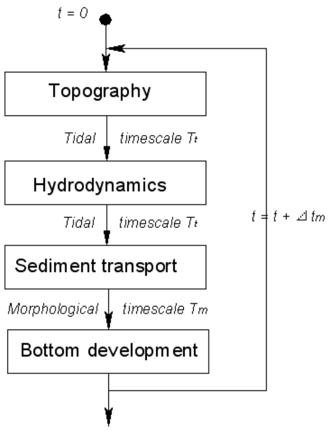

Fig.1 Model structure

2. Model structure: hydrodynamics and sediment transport
Considering (Fig. 1) it has to be noted that the hydrodynamics and sediment motion vary over the short tidal timescale (T_t = 12 h 25 min). The bottom development occurs on the much longer morphological timescale as a result of the net sediment flux after many tidal periods.

This chapter follows the structure of (Fig. 1) and starts with a description of the hydrodynamics. After that the sediment motion is described for uniform and nonuniform sediment.

2.1 Hydrodynamics

For conditions far offshore, the hydrodynamics are dominated by the tidal forcing. This is in contrast with the situation near the coast, where the effect of storms and waves is much more important.

As sketched in (Fig. 2), the total water depth in a coastal sea varies spatially. The spatial coordinates x^* and y^* are in the horizontal direction, z^* is in the vertical direction. Aside from the constant mean water depth H^*, the total water depth is determined by variations in bottom level h^*, occuring on the long morphological timescale, and variations in water surface level z^*.

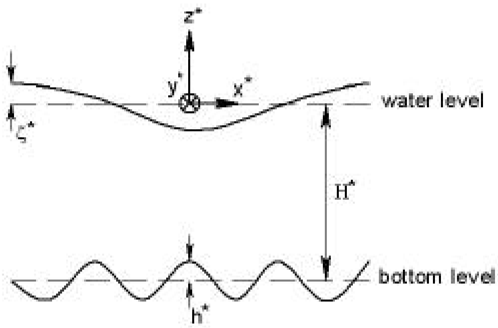

Fig.2 Definition sketch

Scaled 2DH shallow water equations procedure

The model uses the two-dimensional depth-averaged (2DH) shallow water equations to describe the hydrodynamical motion. These equations follow from the Navier-Stokes equations after application of a scaling procedure and the relevant boundary conditions and assumptions, see (Wemmenhove, 2004). The 2DH shallow water equations are given by

$$\frac{\partial u}{\partial t}+u\frac{\partial u}{\partial x}+v\frac{\partial u}{\partial y}-fv+\frac{\partial z}{\partial x}+\frac{ru}{1-h}=0 \tag{1}$$

$$\frac{\partial v}{\partial t}+u\frac{\partial v}{\partial x}+v\frac{\partial v}{\partial y}+fu+\frac{\partial z}{\partial y}+\frac{rv}{1-h}=0 \tag{2}$$

$$\frac{\partial}{\partial x}\left((1-h)u\right)+\frac{\partial}{\partial y}\left((1-h)v\right)=0 \tag{3}$$

In these equations, u and v are the velocity components in the horizontal directions x and y. f (≈ 0.8) is the Coriolis parameter, and r (≈ 0.6) the bottom friction coefficient.

The solution of the hydrodynamical problem, written as the vector $\vec{y}=(u,v,z)$, is not exact. However, it is possible to perform a linear approximation. The vector consists of a basic state and a linear perturbation:

$$\vec{y}=\vec{y}_0+g\,\vec{y}_1+O\left(g^2\right) \tag{4}$$

The bottom topology h is a known variable for the solution of the hydrodynamical problem, since the bottom development occurs on the long morphological timescale and is not determined again after each tidal period. The linear approximation procedure has been described in (Wemmenhove, 2004).

Description of tidal flow

Realistic tidal flow curves describe an elliptical path. However, when the ellipticity is relatively small, it is possible to flatten the elliptical tidal curve to obtain a unidirectional tidal curve (Van der Molen et.al., 2001).

The unperturbed flow velocities for symmetrical and asymmetrical tidal conditions are:

$$(u_0, v_0)=(U_{M2}\sin t, 0) \qquad \text{(symmetrical tide)} \tag{5}$$

$$(u_0, v_0)=(U_{M0}+U_{M2}\sin t+U_{M4}\sin(2t-c), 0) \qquad \text{(asymmetrical tide)} \tag{6}$$

For symmetrical tidal conditions there is only a periodic M2 component (U_{M2}), for asymmetrical tidal conditions there is also a residual current U_{M0} and an M_4 component which introduces a phase difference.

Since sediment transport is proportional to the third power of the flow velocity $\left(q \propto u^3\right)$, asymmetrical tidal conditions result in migration of sandbanks (since the tidally-averaged value of the sediment flux is unequal to zero), in contrast with symmetrical tidal conditions.

2.2 Sediment transport

Sediment characteristics

For a sediment mixture it is convenient to describe the grain diameters using a logarithmic scale. The grain diameter for an arbitrary grain size class i is described on the logarithmic f-scale by

$$\frac{d^{(i)}}{d_{ref}} = 2^{-f(i)}, \qquad d_{ref} = 1 \text{ m} \tag{7}$$

The sediment mixture is represented using only two grain sizes. To generate quantitatively dependable predictions for a test case it would be useful to take more grain sizes, or more grain size distribution parameters, into account. However, for studying the effect of nonuniform sediment qualitatively, a bimodal sediment mixture, consisting of two grain sizes, is likely to satisfy. Each grain size has its own volume fraction, the volume fractions should add up to one. For a bimodal mixture, consisting of grain size fractions $F^{(A)}$ and $F^{(B)}$, this gives

$$F^{(A)} + F^{(B)} = 1 \tag{8}$$

Sediment continuity

Spatial variations in the flow-induced sediment flux q will result in a change of the bottom level h. (Fig. 3) shows the structure of the bottom in the model for uniform and nonuniform sediment.

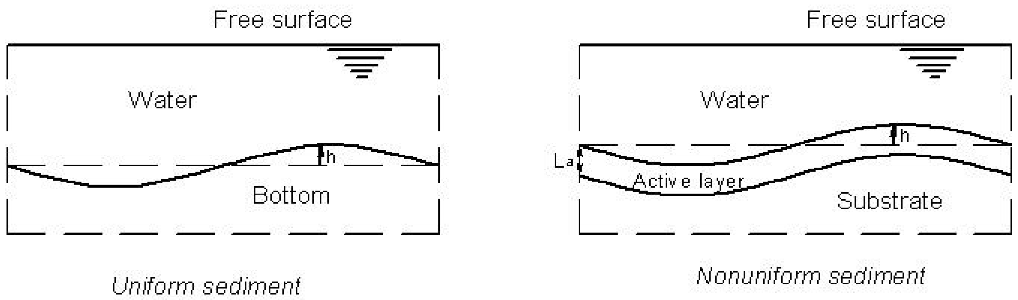

Fig. 3 Sediment continuity for uniform and nonuniform sediment

The fundamental difference between both figures is the presence of an active layer for a bottom consisting of nonuniform sediment (Ribberink (1987), Walgreen (2003)). For nonuniform sediment it is assumed that only the grain size distribution in the active layer is affected by the flow, while the substrate is assumed not to be disturbed. The active layer thickness L_a depends on the average grain size ϕ_m and the standard deviation σ_0 on this average grain size (Walgreen, 2003):

$$L_a = 2^{s_0 - f_m} \tag{9}$$

For uniform sediment the sediment continuity equation relates the bottom development h to spatial variations in the sediment flux q:

$$\frac{\partial h}{\partial t} + \vec{\nabla} \cdot \vec{q} = 0 \tag{10}$$

For nonuniform sediment the sediment continuity equation reads for each grain size fraction $F^{(i)}$:

$$F^{(i)} \frac{\partial h}{\partial t} + L_a \frac{\partial F^{(i)}}{\partial t} + \vec{\nabla} \cdot \vec{q}^{\,(i)} = 0 \tag{11}$$

Sediment flux: uniform sediment

The sediment flux in the model depends on the flow velocity and on variations in bottom level. For conditions far offshore, when the bank height is much smaller than the mean water depth, bedload transport is assumed to be the dominant sediment transport mechanism. For nearshore conditions, and moreover when sandbanks significantly grow towards the water surface level, the importance of suspended transport strongly increases.

For uniform sediment the bedload flux is given by

$$\vec{q}_{unif} = n_b \left(\left|\vec{u}\right|^2 \vec{u} - \left|\vec{u}\right|^3 l \, \vec{\nabla} h \right) \tag{12}$$

In equation (12), ν_b (= $O(10^{-5})$) is the transport parameter and λ ($\approx 5.10^{-3}$) is the bedslope coefficient.

Sediment flux: nonuniform sediment

For nonuniform sediment the total sediment flux can be calculated as the sum of the fluxes of the different grain size classes *i*. The different grain sizes $d^{(i)}$ are not transported just as easily.

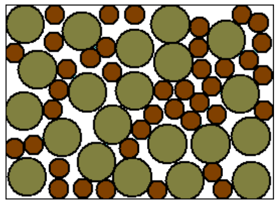

Fig. 4 Bimodal mixture

A bimodal mixture consists of coarse grains A and finer grains B, as sketched in figure 4. The fine grains in a bimodal mixture are more or less protected from movement by the coarse grains, this is the 'hiding' effect. On the other side, the coarse grains are picked up more easily by the flow when they are surrounded by fine grains, this is the 'exposure' effect. Both effects together imply that a volume of fine particles is picked up by the flow less easily than a volume of coarse particles.

The hiding and exposure effects are implemented in the model by the hiding function $G^{(i)}$. For a specific grain size class of grain diameter $d^{(i)}$ the hiding function is given by (Walgreen, 2003):

$$G^{(i)} = \left(\frac{d^{(i)}}{d_m}\right)^{\frac{3}{2}m_b} \tag{13}$$

The parameter m_b is an empirical parameter; to parametrize the hiding effect properly its value should be larger than zero. The variable d_m is the average grain diameter of the sediment mixture.

The sediment flux for an arbitrary grain size class and the total sediment flux are given by

$$\vec{q}^{\,(i)}_{bim} = \alpha^{(i)}\left[\nu_b\left(\left|\vec{u}\right|^2\vec{u} - \left|\vec{u}\right|^3\lambda\vec{\nabla}h\right)\right] = F^{(i)}G^{(i)}\left[\nu_b\left(\left|\vec{u}\right|^2\vec{u} - \left|\vec{u}\right|^3\lambda\vec{\nabla}h\right)\right] \tag{14}$$

$$\vec{q}_{bim} = \sum \vec{q}^{\,(i)}_{bim} = \alpha\left[\nu_b\left(\left|\vec{u}\right|^2\vec{u} - \left|\vec{u}\right|^3\lambda\vec{\nabla}h\right)\right] \tag{15}$$

The value of the transport coefficient α for an example of a sediment mixture is shown in (Fig. 5), using the given hiding parametrization. There are different ways to describe a bimodal sediment mixture. In (Fig. 6), for example, one grain diameter is fixed (either the coarse or the fine diameter) and the average grain diameter is kept constant at d_m = 0.3 mm. Varying the volume fraction of the coarse particles shows that the value of the transport coefficient α is always larger than unity.

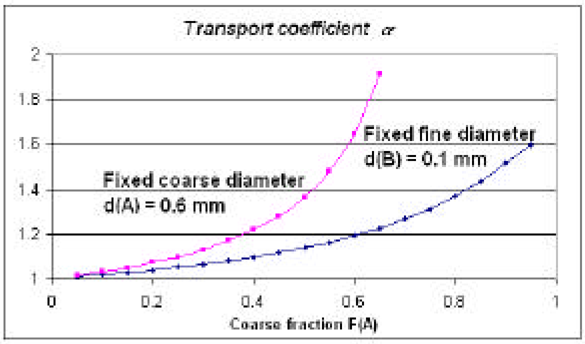

Fig.5 Transport coefficient α for a bimodal mixture

3. Model structure: morphodynamics

The model is restricted to topographies which vary in one horizontal dimension only. This assumption is supported by the predominantly one-dimensional character of sandbank patterns observed in reality.

The development of bed forms occurs on the long morphological timescale T_m, while the motion of water and sediment occurs on the short tidal timescale T_t. The morphological timescale is related to the tidal timescale by the transport coefficient α, it is given by $T_m = T_t/\alpha$. The sediment continuity equations for uniform sediment (15) and for nonuniform sediment (17) have been scaled and linearized in (Wemmenhove, 2004).

3.1 Uniform sediment

After linearization it is possible to give a relation for the amplitude of the bottom development (the maximum bank sandbank height) and the growth rate ω_{unif} in case of uniform sediment:

$$\frac{\partial \hat{h}_1}{\partial t_m} = -\vec{\nabla}\cdot\left\langle \vec{q}_{unif}\right\rangle = \omega_{unif}(k,l)\hat{h}_1 \tag{16}$$

The term $\vec{\nabla}\cdot\left\langle \vec{q}_{unif} \right\rangle$ in equation (16) is the divergence of the tidally-averaged sediment flux. The solution for the growth rate ω_{unif} has been given earlier in (Roos, 2002) and (Wemmenhove, 2004). The growth rate of a sandbank strongly depends on its orientation with respect to the tidal flow, this orientation is indicated by the vector *(k,l)*. The orientation of a sandbank corresponding to the maximum value of the growth rate is the fastest growing mode. For the fastest growing mode the angle between bank crest and principal flow direction depends on the flow conditions and the chosen parameter values in the model, usually the angle lies between 30° and 50°. The wavelength, the distance between two adjacent sandbanks, varies from 5 up to 10 kilometers.

3.2 Nonuniform sediment

For uniform sediment the flow velocity and bottom level did not appear to be spatially constant. For nonuniform sediment there will also be spatial and temporal variations in grain size.
The fraction of each grain size is the sum of the spatially constant fraction $f_0^{(i)}$ and the local perturbation $f_1^{(i)}$ on that average fraction, with a small parameter $\gamma << 1$:

$$F^{(i)}(x,y,t_m) = f_0^{(i)} + g\left(\hat{f}_1^{(i)}(t_m)e^{i(kx+ly)} + c.c.\right) \tag{17}$$

For a bimodal sediment mixture the sum of the grain size fractions should add up to one:

$$f_0^{(A)} + f_0^{(B)} = 1,\ \ f_1^{(A)} = -f_1^{(B)} \tag{18}$$

The hiding function $G^{(i)}$ has an analogous structure:

$$G^{(i)}(x,y,t_m) = g_0^{(i)} + g\left(\hat{g}_1^{(i)}(t_m)e^{i(kx+ly)} + c.c.\right) \tag{19}$$

The perturbed part of the hiding function is given by (Walgreen, 2003):

$$g_1^{(i)} = f_1^{(i)} g_0^{(i)} N = f_1^{(i)} g_0^{(i)} \frac{3m_b s_0 \ln(2)}{\sqrt{F^{(A)}F^{(B)}}} \tag{20}$$

The transport coefficient α, mentioned in equation (14), is also not constant:

$$a^{(i)} = a_0^{(i)} + g a_1^{(i)} = \left(f_0^{(i)} g_0^{(i)} + g\left(f_0^{(i)} g_1^{(i)} + f_1^{(i)} g_0^{(i)}\right)\right) \tag{21}$$

The sediment flux incorporates all linearized variables mentioned above:

$$q_{bim}^{(i)} = q_{bim,0}^{(i)} + g q_{bim,1}^{(i)} = a^{(i)} q_{unif,0} + g\left(a_1^{(i)} q_{unif,0} + a_0^{(i)} q_{unif,1}\right) \tag{22}$$

The divergence of the tidally-averaged sediment flux for a grain size fraction evolves from equations (21) and (22):

$$\begin{aligned} &\vec{\nabla}\cdot\left\langle q_{bim}^{(i)}\right\rangle = \vec{\nabla}\cdot\left\langle q_{bim,1}^{(i)}\right\rangle = \\ &= f_0^{(i)} g_0^{(i)}\, \vec{\nabla}\cdot\left\langle q_{unif,1}\right\rangle + \left\langle q_{unif,0}\right\rangle \vec{\nabla}\cdot\left(f_0^{(i)} g_1^{(i)} + f_1^{(i)} g_0^{(i)}\right) + \left(f_0^{(i)} g_1^{(i)} + f_1^{(i)} g_0^{(i)}\right)\vec{\nabla}\cdot\left\langle q_{unif,0}\right\rangle \end{aligned} \tag{23}$$

The value of $\vec{\nabla}\cdot\left\langle q_{unif,1}\right\rangle$ follows from equation (15), while $\vec{q}_{unif,0} = \left|\vec{u}_0\right|^2 \vec{u}_0$.

Summation of equations (11) gives for both grain size fractions, knowing that $f_1^{(A)} = -f_1^{(B)}$, an expression for the total bottom development:

$$\frac{\partial h}{\partial t_m} = -\left(\vec{\nabla}\cdot\left\langle q^{(A)}\right\rangle + \vec{\nabla}\cdot\left\langle q^{(B)}\right\rangle\right) \tag{24}$$

Back-substitution of equation (24) into equation (11) for grain size fraction *A* gives:

$$L_a \frac{\partial f_1^{(A)}}{\partial t_m} = F^{(A)}\, \vec{\nabla}\cdot\left\langle q_1^{(B)}\right\rangle - F^{(B)}\, \vec{\nabla}\cdot\left\langle q_1^{(A)}\right\rangle \tag{25}$$

The bottom development and changes in grain size composition both depend on the bottom level and grain size fractions. Equations (24) and (25) can be written as:

$$\begin{bmatrix} \dfrac{\partial \hat{h}}{\partial t_m} \\ \dfrac{\partial \hat{f}_1^{(A)}}{\partial t_m} \end{bmatrix} = \begin{bmatrix} PQ \\ RS \end{bmatrix} \begin{bmatrix} \hat{h} \\ \hat{f}_1^{(A)} \end{bmatrix} \tag{26}$$

with:

$$P = n_b \left(f_0^{(A)} g_0^{(A)} + f_0^{(B)} g_0^{(B)} \right) w_{unif} \tag{27}$$

$$Q = -n_b \left\langle \vec{q}_0 \right\rangle \left(g_0^{(A)} \left(1 + f_0^{(A)} N\right) - g_0^{(B)} \left(1 + f_0^{(B)} N\right)\right)(ik + il) \tag{28}$$

$$R = \frac{n_b}{L_a} f_0^{(A)} f_0^{(B)} \left(g_0^{(A)} - g_0^{(B)} \right) w_{unif} \tag{29}$$

$$S = -\frac{n_b}{L_a} \left\langle \vec{q}_0 \right\rangle \left(g_0^{(B)} \left(1 + f_0^{(B)} N\right) + g_0^{(A)} \left(1 + f_0^{(A)} N\right)\right)(ik + il) \tag{30}$$

Symmetrical tidal conditions

For symmetrical tidal conditions (tidal motion with only an M_2 component) the value of $<q_0>$ is equal to zero. This means that for those conditions $Q = 0$ and the bottom development is given by

$$\frac{\partial \hat{h}}{\partial t_m} = P \hat{h}_1 \tag{31}$$

It has been shown in (Wemmenhove, 2004) that, as long as the value of the hiding parameter m_b is larger than zero, the growth rate increases for symmetrical tidal conditions by the introduction of a bimodal sediment mixture (also see (Fig. 5)).

Segregation of grain size fractions

Deriving a space-dependent relation for the grain size composition would make it possible to predict on which parts of sandbanks coarse and fine particles are concentrated.
The bottom topology has the periodic structure

$$h_1 = \hat{h}_1 e^{i(kx+ly)} + c.c. \tag{32}$$

The equation for the developing sediment composition is (see equation (26)):

$$\frac{\partial f_1^{(A)}}{\partial t_m} = R \hat{h}_1 + S \hat{f}_1^{(A)} \tag{33}$$

In previous models (Walgreen, 2003) the left-hand side of equation (33) was neglected, although the system of equations (26) can be solved exact. This neglect is only allowed when the asymmetry of the tide is not too small, a preliminary survey has shown that this is allowed for typical tidal conditions. The topology of the coarse grain fraction is then given by:

$$\begin{aligned} \hat{f}_1^{(A)} &= \left(-\frac{R}{S} \right) h_1 = x \hat{h}_1 = (x_r + i x_i) \hat{h}_1 = \\ &= (-i w_r + w_i) \left(\frac{1}{\langle q_0 \rangle (k + l)} \right) \left(\frac{f_0^{(A)} f_0^{(B)} \left(g_0^{(A)} - g_0^{(B)} \right)}{g_0^{(A)} \left(1 + f_0^{(A)} N\right) + g_0^{(B)} \left(1 + f_0^{(B)} N\right)} \right) \hat{h}_1 \end{aligned} \tag{34}$$

Two quantities are important to quantify the segregation of the grain size fractions.

The phase shift $\chi_{f1,h}$ indicates on which parts of a tidal sandbank the coarse and fine particles are concentrated. The phase shift follows from (34):

$$c_{f1,h} = -\arctan\left(\frac{x_i}{x_r} \right) = \arctan\left(\frac{w_{uni,r}}{w_{uni,i}} \right) \tag{35}$$

The segregation amplitude shows how strong the segregation of grain size fractions will be, it is the height of the peak of $f_1^{(A)}$ in figure 7. The segregation amplitude is given by

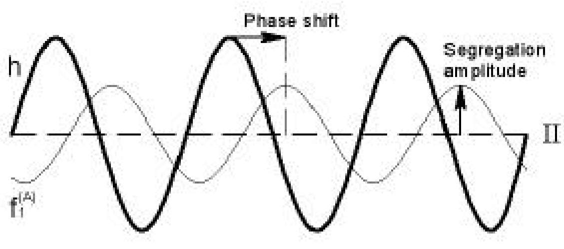

Fig. 7 Phase shift and segregation amplitude

$$\hat{f}_1^{(A)} = \sqrt{x_r^2 + x_i^2}\,\hat{h}_1 \qquad (36)$$

4. Results

The effect of nonuniform sediment on the development of tidal sandbanks and the segregation of different grain size fractions strongly depends on the tidal flow conditions.
For symmetrical tidal conditions the growth rate of sandbanks increases by the introduction of nonuniform sediment, as long as the hiding parameter m_b has a positive value (see (Fig. 5)).
Coarse particles are concentrated on the crests of sandbanks, while fine particles have a tendency to collect in the troughs (see left part of (Fig. 8)).
For more realistic asymmetrical tidal conditions there will be migration of sandbanks, the migration rate is at most several meters each year. The coarse particles are generally concentrated on the lee side of a sandbank (see right part of (Fig. 8)).

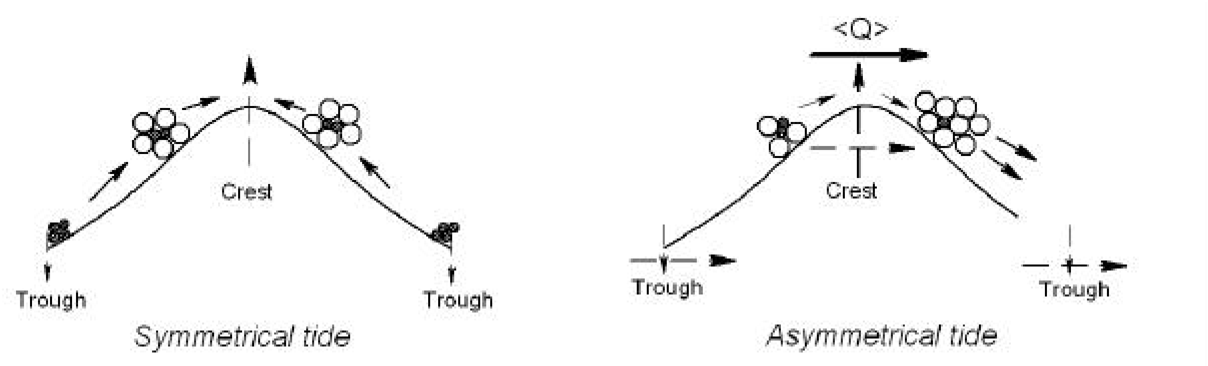

Fig. 8 Particle movement for symmetrical and asymmetrical tidal conditions

The sensitivity of the phase shift and segregation amplitude has been tested for strongly asymmetrical tidal conditions. The sensitivity of the phase shift to a number of scaled model variables is represented in (Fig. 9). The sensitivity of the segregation amplitude to a number of scaled model variables is shown in (Fig. 10). The domain of the variables tested in (Fig. 9) and (Fig. 10) is shown in table 1, together with the default values of the variables.

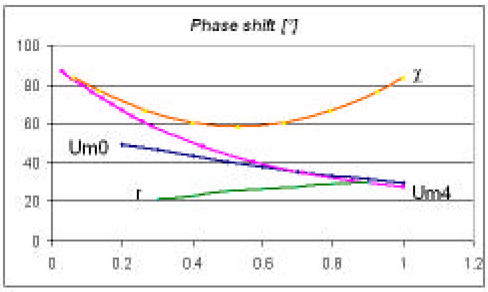

Fig. 9 Phase shift sensitivity; U_{M0}, U_{M4}, c and r on x-axis (see table 1)

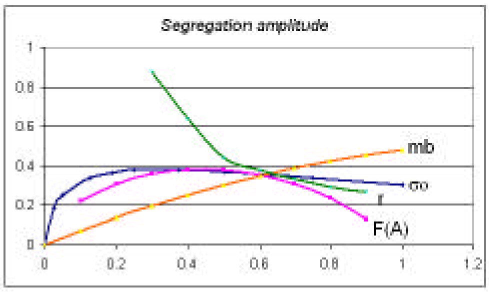

Fig.10 Segregation amplitude sensitivity; r, s_0, F(A) and m_b on x-axis (see table 1)

	x_{min}	x_{max}		*Default value*
U_{m0}	0	0.1	Residual current	0.1 ms^{-1}
U_{m2}	1	1	M2 tidal component	1 ms^{-1}
U_{m4}	0	0.35	M4 tidal component	0.25 ms^{-1}
χ	10	170	M4 phase	90 °
r	0.3	0.9	Friction parameter	0.6
σ_0	0	4	Standard deviation	1
F(A)	0.1	0.9	Coarse fraction	0.5
m_b	0	1	Hiding parameter	0.5

Table 1 List of variables on x-axes in figures 9 and 10

It appears from (Fig. 9) that the phase shift is mainly determined by the values of the different tidal components. The friction coefficient *r* only slightly affects the phase shift.

The model has been tested on different sandbank geometries (Wemmenhove, 2004). For the Dutch Banks the model predicted a phase shift of about 55°, while on the Hinder Banks the coarse particles were predicted to be concentrated near the troughs.

5. Discussion and conclusions

The segregation of grain sizes on different parts of tidal sandbanks is described in this article. The segregation pattern strongly depends on the tidal flow conditions. For symmetrical tidal conditions the coarse particles are concentrated on the crests and the grain size composition is in phase with the bottom. For realistic asymmetrical tidal conditions however the coarse particles are concentrated on the lee slope of a migrating sandbank.

The presented model is a highly idealized model, however the morphodynamics of tidal sandbanks can be predicted to some extent. The effect of different tidal flow conditions and of different sediment mixtures can be studied. Although a sediment mixture of only two grain sizes is studied, the qualitative insight into the morphodynamics will not improve greatly when more grain size distribution parameters are taken into account. For particular test cases however, with detailed grain size characteristics available, the quantitative prediction could be improved by taking more grain sizes and grain size distribution parameters into account.

The model itself has still some significant shortcomings for practical application. It is only applicable when perturbations of the sea bed do not grow too large compared with the mean water depth. The nonlinear effects occuring for large perturbations have been studied by (Roos et.al., 2003). Furthermore, the friction near the sea bed is parametrized by a constant friction parameter r. In reality the bottom friction strongly depends on different parameters, for example the local sediment characteristics. Besides, no threshold value is included in the sediment flux formulation. Implementing a threshold into the sediment flux formulation does not influence the phase shift, however the segregation amplitude decreases when a threshold is included.

For practical applications the model could be useful in clarifying physical processes. It could help in predicting the spatial segregation of different grain sizes, for example after human intervention on the sea bed.

References

A.Blom, A vertical sorting model for rivers with non-uniform sediment and dunes, Ph.D. thesis, University of Twente, The Netherlands, 2003.

S.J.M.H. Hulscher, H.E. de Swart and H.J. de Vriend, The generation of offshore tidal sand banks and sand waves, Cont. Shelf Res., 19, pp. 1285-1330, 1993.

J.M. Huthnance, On one mechanism forming linear sandbanks, Est. Coast. and Shelf Science, 14, pp. 74-99, 1982.

J.S. Ribberink, Mathematical modelling of one-dimensional morphological changes in rivers with non-uniform sediment, Ph.D. thesis, Technical University Delft, The Netherlands, 1987.

P.C. Roos and S.J.M.H. Hulscher, Formation of offshore tidal sand banks triggered by a gasmined bed subsidence, Cont. Shelf Res., 22, pp. 2807-2818, 2002.

P.C. Roos, S.J.M.H. Hulscher and M.A.F. Knaapen, The cross-sectional shape of tidal sandbanks: Modeling and observations, submitted to J. Of Geophys. Res., 2003.

J. van der Molen and H.E. de Swart, Holocene tidal conditions and tide-induced sand transport in the southern North Sea, J. of Geophys. Res., Vol. 106(C5), pp. 9889-9362, 2001.

H.J. de Vriend, Morphological processes in shallow tidal seas, Coastal and Estuarine Studies, 38, pp. 276-301, 1990.

M. Walgreen, Dynamics of sand ridges in coatsal seas: the effect of storms, tides and grain sorting, Ph.D. thesis, Utrecht University, The Netherlands, 2003.

R. Wemmenhove, Modelling the effect of nonuniform sediment on the morphodynamics of tidal sandbanks, MSc. Thesis, University of Twente, The Netherlands, 2004.